DMD Fast Forward. Published on October 21, 2024 as DOI: 10.1124/dmd.124.001824
This article has not been copyedited and formatted. The final version may differ from this version.

Absolute Membrane Protein Abundance of P-gp, BCRP and MRPs in Term Human Placenta Tissue and Commonly Used Cell Systems: Application in PBPK Modeling of Placental Drug Disposition

Zubida M. Al-Majdoub*,¥, Jolien J.M. Freriksen¥, Angela Colbers, Jeroen van den Heuvel, Jan Koenderink, Khaled Abduljalil, Brahim Achour, Jill Barber, Rick Greupink, Amin Rostami-Hodjegan

¥ Authors contributed equally to this work

Centre for Applied Pharmacokinetic Research, University of Manchester, Manchester, UK (Z.M.A.-M., J.B., A.R.-H.); Division of Pharmacology and Toxicology, Department of Pharmacy, Radboud University Medical Center, Nijmegen, the Netherlands (J.J.M.-F; J.V.D.-H; J.K; R.G.); Department of Pharmacy, Radboud University Medical Center, Nijmegen, the Netherlands (A.C.); Certara Predictive Technologies, Sheffield, UK (A.R.-H; K.A.); Department of Biomedical and Pharmaceutical Sciences, College of Pharmacy, the University of Rhode Island, Kingston, Rhode Island, USA (B.A.)

DMD Fast Forward. Published on October 21, 2024 as DOI: 10.1124/dmd.124.001824
This article has not been copyedited and formatted. The final version may differ from this version.

Running title: Transporters Abundance in Human Placenta and Cell Systems

Keywords: Human Placenta, QconCAT, quantification concatemer, quantitative proteomics, transporters, PBPK

* Corresponding author:

- Dr Zubida Al-Majdoub, Centre for Applied Pharmacokinetic Research, the University of Manchester, Stopford Building, Oxford Road, Manchester, UK, email: Zubida.al-majdoub@manchester.ac.uk, + 44 161 306 2580

Number of text pages: 36

Number of figures: 3

Number of tables: 4

Number of references: 42

Number of words in abstract: 250 words

Number of words in the significance statement: 52 words

Number of words in text: 6247 words

DMD Fast Forward. Published on October 21, 2024 as DOI: 10.1124/dmd.124.001824
This article has not been copyedited and formatted. The final version may differ from this version.

Abstract

The placenta acts as a barrier, excluding noxious substances whilst actively transferring nutrients to the fetus, mediated by various transporters. This study quantified the expression of key placental transporters in term human placenta (n=5) and BeWo, BeWo b30, and JEG-3 placenta cell lines. Combining these results with pregnancy physiologically-based pharmacokinetic (PBPK) modeling, we demonstrate the utility of proteomic analysis for predicting placental drug disposition and fetal exposure. Using targeted proteomics with QconCAT standards, we found significant expression of P-gp, BCRP, MRP2, MRP4, and MRP6 in the human placenta (0.05 - 0.25 pmol/mg membrane protein) with only regional differences observed for P-gp. Unexpectedly, both P-gp and BCRP were below the limit of quantification in the regularly used BeWo cells, indicating that this cell line may not be suitable for the study of placental P-gp and BCRP-mediated transport. In cellular and vesicular overexpression systems, P-gp and BCRP were detectable as expected. Vesicle batches showed consistent P-gp expression correlating with functional activity (N-methyl-quinidine (NMQ) transport). However, BCRP activity (Estrone 3-sulfate (E1S) transport) did not consistently align with expression levels. Incorporating in vitro transporter kinetic data, along with placental transporter abundance, into a PBPK model enabled the evaluation of fetal exposure. Simulation with a hypothetical drug indicated that estimating fetal exposure relies on the intrinsic clearances of relevant transporters. To minimize interlaboratory discrepancies, expression data was generated using consistent proteomic methodologies in the same lab. Integration of this data in pregnancy-PBPK modeling offers a promising tool to investigate maternal, placental and fetal drug exposure.

DMD Fast Forward. Published on October 21, 2024 as DOI: 10.1124/dmd.124.001824
This article has not been copyedited and formatted. The final version may differ from this version.

Significance statement

This study quantified the expression of key placental transporters in human placenta and various placental cell lines, revealing significant expression variations. By integrating these data with PBPK modeling, the study highlights the importance of transporter abundance data in understanding and predicting placental drug disposition, essential for maternal and fetal health during pregnancy.

Abbreviations:

ABC transporter, ATP-binding cassette transporter; BCRP, breast cancer resistance protein; FASP, filter-aided sample preparation; LC-MS, liquid chromatography–mass spectrometry,; MRP, multidrug resistance-associated protein; LC-MS/MS, liquid chromatography-tandem mass spectrometry; PBPK model, physiologically based pharmacokinetic model; PK, pharmacokinetics; P-gp, P-glycoprotein; QconCAT, Quantification concatemer.

DMD Fast Forward. Published on October 21, 2024 as DOI: 10.1124/dmd.124.001824
This article has not been copyedited and formatted. The final version may differ from this version.

Introduction

Approximately 80% of pregnant women receive prescription medicines, which may be transported across the placenta to the fetus. Pregnant women are, however, generally excluded from clinical studies (Blehar et al., 2013), and, at least initially, the only available data relevant to fetal exposure come from reproductive toxicity studies in animals. Unfortunately, animal models can have poor translational value, as placentation is highly diverse among mammals (Grigsby, 2016). The need for human-based preclinical models of pregnancy to bridge the gap between preclinical animal studies and first application of the drug in pregnant women is clear.

The placenta regulates the exchange of nutrients, waste products and xenobiotics between mother and fetus. The same mechanisms that transfer essential nutrients from mother to fetus may also transfer compounds that interfere with fetal development (Carter, 2020; Lupattelli et al., 2014). The rate and extent of placental transfer of a compound can, to some extent, be predicted by its physicochemical parameters. Passive diffusion across membranes is one of the relevant processes and small, unionized, lipophilic molecules display the largest diffusion coefficients (Al-Enazy et al., 2017).

Placental transporters and enzymes (Gong et al., 2023; Kammala et al., 2022), however, also influence drug transfer. Efforts to chart these have brought new insights into placental functioning, maternal-fetal transport of drugs and fetal protection (Iqbal et al., 2012). The expression of placental transporters (Dallmann et al., 2019; Han et al., 2018) particularly their functional expression in the (syncytio) trophoblast must be understood in order to make good predictions of placental transfer and, despite considerable effort over the past few years, for many drugs it is

DMD Fast Forward. Published on October 21, 2024 as DOI: 10.1124/dmd.124.001824
This article has not been copyedited and formatted. The final version may differ from this version.

unclear whether placental drug accumulation and/or transfer adds to effective therapy or increases the risk of toxicity in utero (Staud et al., 2012).

The need for good data is exacerbated by poor understanding of the alternatives to drug treatment; it is easy for a clinician to suggest that a pregnant patient avoid the use of OTC painkillers to minimize the chance of harm to the fetus, but if the risk of metabolic imbalance in the mother due to the underlying condition (for example migraine) to the fetus is not known, such advice is potentially flawed.

Currently, there are several in vitro and ex vivo approaches to study placental transfer. Ex vivo human placenta perfusion, where the structural and functional integrity of the placenta is retained, is considered the gold standard to study placental transport at term, as it mimics the in vivo situation most closely. The use of human placental trophoblast cell lines is an attractive approach, as it offers a higher throughput system and does not require access to fresh placental tissue. Commonly used cell lines include the b30 subclone of the BeWo human choriocarcinoma cell line, and JEG-3 cells (Eliesen et al., 2021; Li et al., 2013; Schneider et al., 2022). Likewise, studies in systems that recombinantly overexpress key human placental transporters (e.g., P-gp or BCRP) can also be used to infer overall placental drug transport. An important limitation of the use of cell lines and over expression systems is that they remain poorly characterized in terms of transporter expression.

In vitro to in vivo extrapolation (IVIVE) of drug disposition, requires a comparison of absolute membrane transporter abundance in in vitro systems and in primary placental tissue (Harwood et al., 2022), measured using the same methods under similar conditions (Harwood et al., 2016; Prasad et al., 2019). This allows the incorporation of such data into physiology-based pharmacokinetic (PBPK) models (Abduljalil et al., 2012; Staud et al., 2012). Ultimately, such PBPK models will provide

DMD Fast Forward. Published on October 21, 2024 as DOI: 10.1124/dmd.124.001824
This article has not been copyedited and formatted. The final version may differ from this version.

the means to transform classical animal-based reproductive toxicology studies required for drug development into new approaches that apply in vitro and in silico alternatives to estimate fetal drug exposure and fetal risk (Chang et al., 2022). PBPK models can also assist in designing rational dosing adjustments during pregnancy and in rationalizing intervention-based research in pregnant women in the future (Abduljalil and Badhan, 2020; Ke et al., 2018).

The aim of the present work was to quantify transporters in primary human term placental tissues and in commonly used in vitro model systems, using quantitative proteomic methods. The studied in vitro cell lines were BeWo cells, BeWo b30 subclone, JEG-3 cells, HEK293 cells overexpressing P-glycoprotein (P-gp) or breast cancer resistance protein (BCRP), as well as membrane vesicles derived from P-gp- or BCRP-overexpressing human embryonic kidney (HEK)-293 cells. In addition, an approach of utilizing these data to parameterize a pregnancy PBPK model for a hypothetical drug was demonstrated.

Materials and Methods

Chemicals

Unless otherwise indicated, all chemicals were supplied by Sigma-Aldrich (Poole, Dorset, UK) with the highest purity available. Lysyl endopeptidase (Lys-C) was purchased from Wako (Osaka, Japan), and proteomic-grade trypsin was supplied by Roche Applied Science (Mannheim, Germany) and Promega (Southampton, UK). All solvents were HPLC grade and supplied by ThermoFisher Scientific (Paisley, UK). ProteoExtract native membrane protein extraction kit was purchased from Calbiochem (Temecula, CA).

DMD Fast Forward. Published on October 21, 2024 as DOI: 10.1124/dmd.124.001824
This article has not been copyedited and formatted. The final version may differ from this version.

Human sample sets

Approval of collection of placenta tissue samples was obtained from the Local Ethics Committee on research involving human subjects at Radboud University Medical Center, Nijmegen, Netherlands (file number 2014-1397). After obtaining written informed consent from the donors, placentae from 5 healthy pregnant women were included in this study, and placental tissue was collected after delivery. To assess intra placental variability, 3 samples of villous tissue were taken from different zones of each placenta: one sample from the insertion point of the umbilical cord into the placenta, one from the periphery of the placenta and one sample in between these two points.

Microsomal and cytosolic protein preparation from placental tissue

Frozen placental tissues were thawed, washed, blotted, and weighed. Each placental sample (500 mg) was homogenized and solubilized in 6 volumes of lysis buffer (7 M Urea, 2 M Thiourea, 100 mM Dithiothreitol, 4% (w/v) CHAPS, 10 mM HEPES pH 7.9, 0.1% Octyl β-thioglucopyranoside,1.5 mM $MgCl_2$, 10 mM KCl, and protease inhibitor (complete mini, EDTA free - 1 tablet per 10 ml lysis buffer)) was used to prevent protein degradation; the samples were kept on ice for 2 min. Homogenization was carried out on ice for four bursts of 20s, each with 10s rest (to prevent heating). The lysed cells were kept on ice for 30 min, then centrifuged twice at 800 g at 4°C for 5 min to remove debris. The supernatant was collected and centrifuged at 10,000 g at 4°C for 10 min to remove mitochondrial contamination. The supernatant was then centrifuged in an Optima Ultracentrifuge (Beckman Coulter, CA) for 75 min at 125,000 g at 4°C to generate cytosolic and membrane fractions (pellet). Protein concentrations of both total membrane and cytosolic

DMD Fast Forward. Published on October 21, 2024 as DOI: 10.1124/dmd.124.001824
This article has not been copyedited and formatted. The final version may differ from this version.

fractions were determined using the Bradford protein assay (Bio-Rad). The final protein samples were stored at -80°C prior to LC-MS/MS.

Production of cells and membrane vesicles overexpressing the efflux transporters (P-gp and BCRP)

(1) HEK293 overexpressing P-gp or BCRP

After cloning BCRP or P-gp behind a cytomegalovirus (CMV) promotor into a Baculovirus, HEK293 cells were transduced with these viruses and harvested by centrifugation, as described earlier (Wittgen et al., 2012). Transductions may be less or more efficient, resulting in variable activity of the transporter in the HEK293 cells. To estimate the degree of this variability, 3 batches of cells were transduced with 3 different batches of Baculovirus (per transporter). In this way, 3 independent batches per transporter were created. HEK293 cells were cultured for 4 days in Dulbecco's Modification of Eagle's Medium (DMEM) supplemented with glutamax, including 10% fetal calf serum (FCS). No antibiotics were added to the culture medium. When harvesting, cells were detached via mechanical manipulation (i.e., tapping the culture flask multiple times against the lab bench) and no trypsin was used to detach the cells. Each harvested cell suspension was transferred to a 50 ml falcon tube after which the cells were centrifuged to create a cell pellet, containing $7x10^6$ cells per pellet. The pellets (3 batches of cells overexpressing human P-gp, and 3 batches of cells overexpressing BCRP) were washed twice with ice-cold phosphate buffered saline (PBS) and were stored at -80°C until analysis.

(2) Trophoblast cell lines (BeWo, BeWo b30, JEG-3) cell lines

BeWo cells and JEG-3 cells were obtained from ATCC https://www.atcc.org/.

The BeWo b30 subclone was kindly provided by Dr. Burki (EMPA, St Gallen, Switzerland). BeWo cells (1 batch) and BeWo b30 cells (1 batch) were cultured in DMEM glutamax/F12K (1:1). JEG-3 cells (1 batch) were maintained in DMEM

DMD Fast Forward. Published on October 21, 2024 as DOI: 10.1124/dmd.124.001824
This article has not been copyedited and formatted. The final version may differ from this version.

containing glutamax. All culture media were supplemented with 1% penicillin/streptomycin and 10% fetal calf serum (FCS). When culturing was complete, cell layers were washed once with PBS before harvesting, followed by centrifugation to create a pellet which was stored at -80°C until analysis. The final number of cells obtained after culturing, per batch of BeWo, BeWo b30 or JEG-3 was determined to be $4.5x10^7$, $8.7x10^7$ and $5.2x10^7$ cells, respectively.

(3) Membrane vesicles overexpressing P-gp or BCRP

Membrane vesicles overexpressing P-gp or BCRP were produced from HEK293 cells overexpressing these transporters, as described earlier (Wittgen et al., 2012). Membrane vesicles are a common system for the study of drug transport by ATP-binding cassette (ABC) transporters. These samples were included in our proteomic analysis. In brief, transduced HEK293 cells were harvested by centrifugation. The 100,000 g membrane fraction was homogenized in ice-cold TS buffer (10 mM Tris-HEPES and 250 mM sucrose, pH 7.4) and high shear passage through a 100 µm opening was used to prepare membrane vesicles. The vesicles were dissolved in a buffer containing 20 mM Tris and 500 mM sucrose, and HEPES was used to set the pH at 7.4. Vesicles were snap frozen in liquid nitrogen and stored at -80°C, prior to use. Protein concentration of vesicles was determined using a Bradford assay.

To verify functional expression of membrane transporters in the membrane vesicles, transport assays were conducted prior to proteomic analysis. Briefly, 30 ml reaction mix containing TS buffer, 10 mM $MgCl_2$, 4 mM AMP or ATP and 7.5 µg pre-warmed (37ºC) vesicles preparations were supplemented with 0.1 µM N-methyl quinidine (NMQ) to measure P-gp activity and 0.1 µM estrone-sulfate (E1S) to measure BCRP activity. The reaction was started by incubation of the samples at 37ºC and was stopped by transferring the samples on ice and adding 150 µl of ice-cold TS buffer.

DMD Fast Forward. Published on October 21, 2024 as DOI: 10.1124/dmd.124.001824
This article has not been copyedited and formatted. The final version may differ from this version.

The diluted samples were filtered through a TS-prewashed 0.65-µm pore, 96-well Multiscreen HTS glass fiber filter plate using a Multi-screenHTS-Vaccum Manifold filtration device (Millipore, Etten- Leur, The Netherlands). After washing the filters with TS buffer twice (0.2 ml), samples were processed for NMQ or E1S analysis, as described previously (Wittgen et al., 2012).

Preparation of membrane protein from cell lines (BeWo, BeWo b30, JEG-3 cells and HEK293)

All cell lines were similarly processed using ProteoExtract native membrane protein extraction kit (Calbiochem), following the manufacturer's protocol with minor modifications, to isolate total membrane proteins. Briefly, the cells were washed with 2 ml ice cold wash buffer, then centrifuged at 100-300 g at 4°C for 10 min. The pellets were lysed in 2 ml of extraction buffer I of the kit, containing protease inhibitor cocktail (10 µl), and incubated with gentle shaking for 10 min. The resultant homogenate was centrifuged at 16,000 g for 15 min. The pellet was resuspended in 1 ml of extraction buffer II of the kit with 5 µl of protease inhibitor cocktail. The fraction was incubated with gentle shaking for 1.5 h at 4°C, followed by centrifugation at 16,000 g for 15 minutes at 4°C. The supernatant, containing membrane fraction enriched in integral membrane and membrane-associated proteins, was collected, and the total isolated membrane protein concentration was determined using a Direct Detect® Spectrometer. The procedure was the same for all cell lines, but the volume of the reagents used was scaled according to the number of cells lysed.

Sample preparation for proteomic analysis

Placentae and cell lines (including membrane vesicles) protein digestion were prepared using the Filter-Aided Sample Preparation (FASP) as described previously (Al-Majdoub et al., 2019; Russell et al., 2013). Briefly, 0.12 µg of TransCAT

(QconCAT for the quantification of transporters) (Russell et al., 2013), used for targeted quantification, was spiked in 50 µg of each individual sample as internal standard. Details of sample preparation protocols and peptide desalting are described in our previous work (Al-Majdoub et al., 2019).

Parallel Reaction Monitoring (PRM) assays and targeted LC−MS/MS analysis for placental tissues and cell lines

Microsomal, cytosolic proteins and cell lines were analyzed by LC−MS/MS using a Thermo RSLC system consisting of a NCP3200RS nano pump, WPS3000TPS autosampler and TCC3000RS column oven configured with buffer A as 0.1% formic acid in water and buffer B as 0.1% formic acid in acetonitrile. An injection volume of 2 µl was loaded into the end of a 5 µl loop and reversed flushed onto the analytical column (Waters nanoEase M/Z Peptide CSH C18 Column, 130Å, 1.7 µm, 75 µm x 250 mm) kept at 35°C at a flow rate of 300 nl/min with an initial pulse of 500 nl/min for 0.1 min to rapidly re-pressurise the column. The separation consisted of a multistage gradient of 1% B to 6% B over 3 minutes, 6% B to 18% B over 67 minutes, 18% B to 29% B over 9 minutes and 29% B to 65% B over 1 minute before washing for 6 minutes at 65% B and dropping down to 2% B in 1 minute. The complete method time was 120 minutes. The analytical column was connected to a Thermo Exploris 480 mass spectrometry system via a Thermo nanospray Flex ion source via a 20 µm ID fused silica capillary. The capillary was connected to a fused silica spray tip with an outer diameter of 360 µm, an inner diameter of 20 µm, a tip orifice of 10 µm and a length of 63.5 mm (New Objective Silica Tip FS360-20-10-N-20-6.35CT) via a butt-to-butt connection in a steel union using a custom-made gold frit (Agar Scientific AGG2440A) to provide the electrical connection. The nanospray voltage was set at 1900 V and the ion transfer tube temperature set to 275°C.

DMD Fast Forward. Published on October 21, 2024 as DOI: 10.1124/dmd.124.001824
This article has not been copyedited and formatted. The final version may differ from this version.

Data acquisition, analysis and protein quantification

Data were acquired in Retention Time Window mode, with an expected peak width of 15 seconds, and no full MS data acquired. The target list of TransCAT peptides (El-Khateeb et al., 2021; Vasilogianni et al., 2022) were imported into the method via an Excel .csv file, which included their previously determined retention times, with a retention time window of 4 minutes. Fragmentation spectra were acquired with a resolution of 15,000 with a normalized collision energy of 30%, the AGC target set to Standard, and a max fill time of 100 ms for a single microscan. All data were collected in profile mode. Skyline version 22.2 software (MacCross Lab Software, Seattle, WA) used for generation of the abundance data, as previously described (Al-Majdoub et al., 2019).

Statistical data analysis

Microsoft Excel 2016 and GraphPad version 10.3.0 (La Jolla, CA) were used for statistical analysis. When multiple groups were compared one-way ANOVA was performed, followed by the Tukey's post-hoc test. When two groups were compared, this was done via the Student's unpaired, 2-tailed, t-test, assuming equal variances. A P value cutoff of 0.05 was considered for statistical significance. Differences between expression levels in 5 placentae and across the 3 sites were assessed using the Kruskal-Wallis test. Abundance data were presented as mean and SD, as a measure of interindividual variability. CV was used to describe variability.

In vitro to in vivo extrapolation (IVIVE) of drug transport using vesicles overexpressing a single transporter as a starting point

Overexpression systems offer potential means for extrapolating drug transport kinetics mediated by a specific transporter from in vitro to in vivo. Expression of the

DMD Fast Forward. Published on October 21, 2024 as DOI: 10.1124/dmd.124.001824
This article has not been copyedited and formatted. The final version may differ from this version.

studied transporters was measured in cell models. These expression values were then scaled to be utilized in pregnancy PBPK models as described below.

In vesicular systems, transport by ABC-transporters was measured in the direction from the incubation buffer towards the interior of the vesicles, as only the inside-out folded vesicles (and not the right-side out folded fraction of the vesicles) contribute to transport. The advantage is that the fraction of the transporters contributing to transport is directly exposed to the drug from the incubation buffer. Therefore, transport rate can be related directly to the unbound concentrations present in the incubation buffer to calculate intrinsic transport clearance (CL_{intT}) in a straightforward manner. A stepwise approach is as follows:

1. The intrinsic transport clearance of a drug measured in vesicles specifically over-expressing a single human ABC-transporter ($CL_{intT,\ tot}$), is a composite of active and passive transport. To separate the active from the passive transport clearance in this system, a second set of control experiments are performed in vesicles that do not overexpress the specific transporter, but a control protein instead, e.g. Enhanced Yellow Fluorescent Protein (EYFP). The degree of passive transport clearance (CL_{dif}) that contributes to $CL_{intT,\ tot}$ can thus be derived from these EYFP-expressing vesicles.

2. To calculate an intrinsic active transport clearance from the vesicles that over-express the transporter of interest, CL_{dif} shall be subtracted from $CL_{intT,\ tot}$, yielding an active intrinsic transport clearance $CL_{intT,\ raw}$ expressed as µl/min/mg total vesicular protein present in the in vitro system.

DMD Fast Forward. Published on October 21, 2024 as DOI: 10.1124/dmd.124.001824
This article has not been copyedited and formatted. The final version may differ from this version.

3. To conduct IVIVE based on membrane transporter abundance, this value should be first converted to an intrinsic transport clearance per mg of membrane protein present in vitro. Although for cellular systems, this may be a relevant intracellular protein fraction, for vesicles, it was assumed that all protein to be membrane bound, hence in this case:

$$CLintT, membr = CLintT, raw$$

Where $CL_{inT,\ membr}$ is the intrinsic transport clearance per amount of vesicular membrane protein (expressed as µl/min/mg membrane protein vesicle).

4. The $CLintT, membr$ was then converted to an initial $CL_{inT\ init}$, expressed in µl/min/pmol of transporter that was overexpressed in the membrane, by taking into account the number of picomoles of a specific Transporter that was present per mg Vesicular Membrane Protein (TpVMP), as measured in the proteomics procedure.

$$CLintT, init = \frac{CLintT, membr}{TpVMP}$$

5. Vesicles used for the measurement of in vitro transport rates generated from HEK293 cells are generally 50% right-side out and 50% inside-out, because of the way these vesicles fold during preparation. Only the inside-out vesicles contribute to the active transport observed in the in vitro assay, as only these will have the ATP binding site exposed to ATP present in the incubation buffer. Diffusion of the very hydrophilic ATP into right-side out vesicles, which would be required to activate that fraction of the transporters, is negligible. Since only half of the vesicles, i.e., 50% of

DMD Fast Forward. Published on October 21, 2024 as DOI: 10.1124/dmd.124.001824
This article has not been copyedited and formatted. The final version may differ from this version.

the transporters that were quantified by proteomics are active in the assay, the $CL_{intT,init}$ was corrected to yield a final CL_{intT} (i.e., divide by 0.5):

$$CLintT = \frac{CLintT, init}{0.5}$$

6. The Simcyp® PBPK model (Version 23, Certara Predictive Technologies, Sheffield, UK) utilizes the measured absolute expressions of these transporters in term placentae together with the experimental value for the transporter intrinsic clearance obtained from the vesicle system, using the following IVIVE approach.

$$CLu_{intT}\left(\frac{L}{h}\right) = \frac{CL_{intT}(uL/min/pmol)}{fu_{inc,T}} \cdot AbsolAbund_{T,x}(pmol/g\ of\ placenta) \cdot PlacentaWT_x(g) \cdot SF \cdot \frac{60}{1000000}$$

where CL_{intT} is the in vitro intrinsic clearance in µL/min/pmol of the transporter, $AbsolAbund_{T,x}$ is the absolute expression of transporter abundance in the placenta in pmol per gram of the placental weight ($PlacentaWT_x$) at term. The *SF* is the scaling factor for the transporter with respect to the abundance per phenotype (SF = 1 for subjects carrying the wild-type phenotype of the transporter of interest, i.e., extensive transporter). The $fu_{inc,T}$ is the free fraction of the drug in the *in vitro* incubation, assumed to be 1. The scaled transporter unbound intrinsic clearance (CLu_{intT} in L/h) is then used in the PBPK model equations for placenta transport. The following equation describes the change of drug concentration in the maternal placental compartment:

DMD Fast Forward. Published on October 21, 2024 as DOI: 10.1124/dmd.124.001824
This article has not been copyedited and formatted. The final version may differ from this version.

$$V_{pl}^{m}(t)\frac{dC_{pl}^{m}}{dt} = Q_{pl}^{m}(t)\cdot\left(C_{art}^{m}-C_{pl}^{m}\right)+CL_{PDM}\cdot\left(Cu_{IW,pl}^{tiss}-Cu_{pl}^{m}\right)+\sum CLu_{int,T,efflux}^{m}\cdot Cu_{IW,pl}^{tiss}$$

where V and C represent the volume and concentration of compartments, respectively. Passive permeability from the maternal side to the placenta is represented as CL_{PDM} and $CL_{u\ m,int,T,efflux}$ represents the intrinsic unbound clearance of an efflux transporter. Compartments are represented as follows: $\frac{m}{pl}$, maternal placenta; $\frac{m}{art}$, maternal arterial blood; $\frac{tiss}{IW.pl}$, intracellular water placental tissue. Maternal plasma fraction unbound (fu) is used to calculate the unbound concentration in the maternal placental compartment (Cu_{pl}^{m}).

For the placental tissue compartment:

$$V_{IW,pl}^{tiss}(t)\frac{dC_{IW,pl}^{tiss}}{dt} = CL_{PDM}\cdot\left(Cu_{pl}^{m}-Cu_{IW,pl}^{tiss}\right)+CL_{PDF}\left(Cu_{pl}^{f}-Cu_{IW,pl}^{tiss}\right)-\sum CLu_{int,T,efflux}^{m}\cdot Cu_{IW,pl}^{tiss}$$

Where a placental intracellular water fu, predicted by default according to the Rodgers and Rowland method (Rodgers and Rowland, 2006), was used to calculate the unbound concentration in the placental tissue compartment ($Cu_{IW,pl}^{tiss}$). *PI*:

DMD Fast Forward. Published on October 21, 2024 as DOI: 10.1124/dmd.124.001824
This article has not been copyedited and formatted. The final version may differ from this version.

placenta; *m*: maternal; *f*: fetal; *tiss*: placental tissue; *art*: arterial blood; *IW*: intracellular; *V:* volume; *C*: concentration; CL_{PDM} and CL_{PDF} for the passive placental permeability clearance for maternal side to placenta and fetal side to placenta, respectively. Details of the model equations have been described earlier (Abduljalil et al., 2022; Zhang et al., 2017; Zhang and Unadkat, 2017).

Simulation of a hypothetical exposure scenario

To illustrate how in vitro CL_{intT} data may be used in combination with placental transporter abundance to predict placental transfer, an exposure scenario was simulated for a hypothetical drug within the Simcyp Simulator, starting off with in vitro transport data generated for BCRP and P-gp mediated transport as they would typically be generated in a vesicular in vitro system. The data were analyzed according to the stepwise approach outlined in the previous section.

1. Measured from in vitro experiments, the following values were assumed: $CL_{intT,\ tot}$ P-gp = 226 µl/min/mg total vesicular protein and $CL_{intT,\ tot}$ BCRP = 266 µl/min/mg total vesicular protein. Passive permeability (CL_{dif}) observed in EYFP-expressing controls vesicles: CL_{dif} = 5.7 µl/min/mg total vesicular protein.

2/3. For this drug, this yields a $CL_{intT,raw}$ of 220.3 µl/min/mg total vesicular protein for P-gp and 260.3 µl/min/mg total vesicular protein for BCRP. Assuming all protein measured in the vesicles is membrane-bound, these are also the corresponding $CL_{intT,\ membr}$ values.

4/5. Next, this value was converted to an initial $CL_{intT\ init}$, which is a clearance expressed in µl/ min/pmol transporter that was overexpressed in the membrane. This

DMD Fast Forward. Published on October 21, 2024 as DOI: 10.1124/dmd.124.001824
This article has not been copyedited and formatted. The final version may differ from this version.

is done by considering the number of picomoles of a specific Transporter that was present per mg Vesicular Membrane Protein (TpVMP), as measured in the proteomics procedure. In Table 2, it can be seen that the values differ between batches. For simplicity, for both, the average value was used for subsequent calculations.

Mean TpVMP P-gp = 4.6 pmol/mg vesicular membrane protein

Mean TpVMP BCRP = 14.4 pmol/mg vesicular membrane protein

Dividing the $CL_{intT,\ raw}$ values by the TpVMP values, yields the $CL_{intT,\ init}$ values. Also correcting for the inside-out fraction of the vesicles (divide by 0.5) yields the corresponding CL_{intT} of 95.8 µl/ min/pmol P-gp and a CL_{intT} of 36.2 µl/min/pmol BCRP. These values can be used for Simcyp parametrization. The model also requires input of placental membrane transporter abundance, expressed as pmol/gram of placental tissue (see Table 4). Note that the abundance of transporters in placental membranes (pmol/mg membrane protein) is as listed in Table 1. Next, simulations were performed in Simcyp, using the input data described in Table 4.

For all simulations, the default virtual Sim-Pregnancy population of 200 pregnant women aged 18-45 years at 38 weeks of gestation (as the transporter abundances were measured in term placenta) was used. A template compound file was used and incorporated values observed for the well-known model substrates of P-gp (NMQ) and BCRP (E1S) for this hypothetical drug: $CL_{int,tot}$ values of 226 and 266 µl/min/mg total vesicular protein, for P-gp and BCRP, respectively. Passive permeability (CL_{dif}) was set at 5.7 µl/min/mg total vesicular protein (based on the experimental value observed for E1S). These estimates were calculated from the data listed in Table 3,

DMD Fast Forward. Published on October 21, 2024 as DOI: 10.1124/dmd.124.001824
This article has not been copyedited and formatted. The final version may differ from this version.

by averaging the values listed per batch and dividing the mean transport rates by the nominal substrate concentration that was tested (0.1 pmol/µl). For passive permeability across the placenta, it was assumed that a medium passive diffusion permeability of 3.1 L/h across the placenta to examine the impact of placental efflux transporters. This was done by assuming a small value of 0.005 L/h/mL placenta for CL_{PDM} and assigning the same value for CL_{PDF} parameters in the model to describe the permeability of the drug in both directions across the placental membrane. The average placenta volume at 38 weeks of gestation is about 620 mL (Abduljalil et al., 2012). The simulation was executed assuming 100 mg of a hypothetical drug, as constant intravenous infusion over 24 h. A second simulation was performed without taking transporter activity into account. Since the impact of the efflux transporters localized on the maternal side of the placenta depends on how much drug is available in the intracellular compartment of the placenta via the passive diffusion, two additional simulations were run by varying the passive diffusion value 10-fold higher and 10-fold lower, while retaining the placental transporter clearance as per the initial scenario.

Results

A QconCAT-based proteomic assay was successfully used to quantify the abundance of several membrane transporters in 5 placenta samples and associated cell lines. The abundance data were used in a PBPK model for IVIVE-based prediction of fetal drug exposure.

Abundance of ABC transporters in the human placenta in three placental sites

QconCAT-based targeted proteomics method was used to quantify six transporters (P-gp, BCRP, multi drug resistance protein-2 (MRP2), MRP3, MRP4, MRP6) and one plasma protein marker ATP1A1 (Na+/K+ ATPase) in 5 individual samples

DMD Fast Forward. Published on October 21, 2024 as DOI: 10.1124/dmd.124.001824
This article has not been copyedited and formatted. The final version may differ from this version.

(Figure 1A and 1B). Table 1 summarizes the protein expression levels. The quantification was performed by parallel reaction monitoring (PRM) with the same specific peptides from the Liver TransCAT used in our previous report (Al-Majdoub et al., 2021; Vasilogianni et al., 2022)**.** From our analysis, the transporters exhibited similar abundance levels (Figure 1A and 1B) in all placentae except the expression of MRP6 was found to be significantly different across all placentae (Kruskal-Wallis test, P = 0.026) (Table 1, Figure 1B). Large interindividual variation is observed in the measured abundances of both the transporters and the plasma membrane marker (ATP1A1), which was included in our study as a housekeeping protein. By measuring the ATP1A1, we were able to examine not only the expression levels of our target proteins but also the potential biological variability of ATP1A1 itself across different samples (Table 1).

Site-dependent variability in placental transporter abundance

Transporter protein abundance in three sites was measured (Figure 1A and 1B). Our analysis revealed a significant variation in the expression of P-gp across different placental sites, as determined by the Kruskal-Wallis test (P = 0.008). This indicates that P-gp expression is not uniform throughout the placenta. In contrast, the expression levels of other transporters (BCRP and MRPs) showed no significant differences across the various placental sites, suggesting a more consistent distribution (Table 1).

Comparative levels of transporter protein expression in HEK293 cells overexpressing P-gp or BCRP, and cultured trophoblast BeWo, BeWo b30 and JEG-3 cells

Protein expression of P-gp and BCRP was measured by LC-MS/MS in various placental cell lines (Table 2). In addition, expression was measured in HEK293 cells,

DMD Fast Forward. Published on October 21, 2024 as DOI: 10.1124/dmd.124.001824
This article has not been copyedited and formatted. The final version may differ from this version.

overexpressing these specific transporters. For HEK293 cells overexpressing P-gp or BCRP, expression levels were compared across three independently generated batches. For P-gp, expression was highest in HEK293, and was approximately 20- and 40-fold greater than P-gp expression in BeWo b30 and JEG-3 cells, when comparing the overall mean ± SD of the 3 HEK P-gp batches to the values found for BeWo b30 and JEG-3, respectively (Table 2).

In all of the 3 separate batches of HEK-P-gp cells, this difference reached statistical significance compared to BeWo b30 and JEG-3 cells, as well as when comparing the overall mean of the 3 batches to the observed values for P-gp in BeWo b30 and JEG-3 cells. The difference in expression of P-gp between BeWo b30 cells and JEG-3 cells did not reach statistical significance. Expression of P-gp in regular BeWo cells was below the limit of quantification (LOQ; 0.02 ± 0.01 pmol/mg protein) hence no ratio or level of statistical significance were calculated compared to the other cells.

When comparing the expression levels of BCRP observed in the HEK overexpression system to those observed in BeWo b30 cells, we found that BCRP expression in BeWo b30 cells was not statistically significant. No difference were observed in BCRP expression between BeWo b30 and JEG-3 cells. Again, the expression of BCRP in regular BeWo cells was below the limit of quantification (LOQ) and hence no ratio or level of statistical significance were calculated. On average, the overall mean levels of overexpressed BCRP in the HEK293 cells appeared lower than those for P-gp in HEK293 cells (Table 2) but this did not reach statistical significance. Also, when comparing expression of P-gp and BCRP within a cell line, there were no statistically significant differences found between transporters.

Abundance of P-gp and BCRP transporters in membrane vesicles

DMD Fast Forward. Published on October 21, 2024 as DOI: 10.1124/dmd.124.001824
This article has not been copyedited and formatted. The final version may differ from this version.

For the membrane vesicles, the expression of P-gp and BCRP transporters levels were compared across 3 batches which overexpressed either one of the two transporters. The measured abundances are presented in Table 2. Expression of BCRP was high in membrane vesicles (average with SD: 14.4 ± 8.55 pmol/mg membrane protein) and on average more than threefold greater than P-gp (average with SD: 4.57 ± 0.67 pmol/ mg membrane protein), but this did not reach statistical significance. Variation in P-gp expression across batches was low, while for BCRP it appeared that one batch had a substantial lower expression of the transporter compared to the other two batches. Transport studies using NMQ (for P-gp) or E1S (for BCRP) were conducted to evaluate the functional activity of these transporters in vesicles. Consistent with the expression data, P-gp showed consistent NMQ transport across all batches (Table 3). However, the transport activity of BCRP varied among batches (Table 3). Specifically, BCRP in batch one exhibited the lowest transport activity, aligning with the expression data (Tables 2 and 3). However, the activity of batches two and three did not correlate with their respective expression levels (Table 3). Batch two, despite showing higher BCRP expression, displayed a contradictory trend in activity.

Simulation of the effect of including transporter kinetics and placental abundance in fetal exposure simulations

Inclusion of transporter kinetics and placental abundance of relevant transport proteins (measured in both placental tissue and in vitro systems (membrane vesicles) using proteomics) in fetal and placental exposure predictions results in significantly different estimations of placental and fetal exposure (Figure 2). Notably, maternal exposure is not affected, while placental and fetal exposure were highly reduced when efflux transporters were included in the predictions. Figure 3 shows a

sensitivity analysis of the impact of passive diffusion on maternal, placental and fetal exposure. The analysis illustrates a considerable effect of passive diffusion clearance on drug concentration in the placenta and umbilical venous blood.

Discussion

Examining the impact of placental transporters function on drug disposition is essential for assessing potential drug exposure of the fetus during pregnancy. In vitro models offer a convenient and high-throughput approach to study potential placental xenobiotic metabolism and transport. However, it is important to note that cell lines may not accurately reflect the diverse cellular composition of the placenta with their unique cellular characteristics. Therefore, selecting the most appropriate model that closely aligns with the specific research question is of utmost importance. The latter is a necessary but not sufficient element and quantitative extrapolation of results is also an important step.

Assessment of placental cell lines at the mRNA level has previously been conducted to determine their usefulness in examining placental functions (Msheik et al., 2019). Nevertheless, mRNA data frequently exhibits limited correlation with protein levels and function, attributed to factors such as post-translational modifications and mRNA instability (Christopher et al., 2022). In contrast, proteomics data demonstrates a stronger correlation with protein activity, including functions such as metabolism and transport activity, offering valuable insights into the functional aspects of biological processes (Monti et al., 2019).

While other researchers (Gil et al., 2005; Mathias et al., 2005; Meyer zu Schwabedissen et al., 2006; Sun et al., 2006) have previously measured the

abundance of placental transporters, using Western blotting and ELISA, or applied qPCR for assessing transporter mRNA expression, these approaches present certain limitations (Goetzl et al., 2022; Nishimura and Naito, 2005). Part of this relates to the temporal changes of mRNA in tissue due to short half-life, whilst cell-free RNA shed in exosomes into circulation is more stable and may correlate better with actual expression of the protein in the target tissue (Achour and Rostami-Hodjegan, 2022).

Current knowledge on protein expression of placental transporters is limited to one study (Anoshchenko et al., 2020) using LC-MS/MS. In our study, a targeted-QconCAT based quantitative proteomics approach was performed to measure the abundance of several efflux transporters (P-gp, BCRP, MRPs), including transporters that had not

been measured before (i.e., MRPs). Furthermore, the expression of P-gp and BCRP transporters in different placental cell lines was measured. All the protein measurements were achieved using LC-MS/MS. The zonal expression of transporters in the placentae was also assessed. Our findings are consistent with a previous study (Anoshchenko et al., 2020), with no notable distinctions observed in transporter expression in various locations, except for P-gp, which showed a significant variation across various sites. This lack of variability and independence from the placenta site was reported before and suggests a uniform distribution of transporters across the placenta (Memon et al., 2014). One of the placentae, however, displayed greater variability (%CV) in the expression of the studied transporters compared to the other four placentae. The most significant variations in the abundance were observed among MRPs specifically in placenta 5, while the levels of P-gp and BCRP proteins were similar across all 5 placentae (Table 1). It is

worth mentioning that the sample size was limited, and our study exclusively focused on term placenta samples. Nevertheless, it is important to note that the methodology employed has been thoroughly established over years within the group.

The abundance data, as well as in vitro vesicular transport data for a hypothetical drug, was used as an exploratory modeling scenario. We used a vesicular system as this is a very common test system used in in vitro drug transport studies, as vesicles (once generated) can be easily stored at -80 C and used when needed without the need for continuously culturing cells, or having to start a new culture of cells first when a question concerning drug transport arises. For BCRP and its model substrate E1S, we noted a discrepancy between the observed transport rates and measured protein BCRP abundance. Assuming measurements of transporter activity and protein abundance are correct, a possible explanation for the mismatch could be that part of amounts of BCRP that were measured in vesicle batch 1 and 2, was less functional compared to the functionality of transporter protein expressed in vesicle batch 3, e.g. due to misfolding of the protein or as a result of a loss of protein function as a result of slightly different conditions in the preparation procedure of this batch of vesicles. Whether this is common or not for the vesicles produced via this method, we do not know, as this is a first comparison between activity and absolute abundance.

This aimed to describe the required steps for incorporating these results within a PBPK approach to estimate placental transporter kinetics and to simulate drug concentration in the placenta and in the umbilical cord.

Simulation results indicated the relevance of acquiring data on efflux transport when estimating fetal exposure, as results heavily depended on the value of transporter intrinsic clearances used. With the assumed, but pharmacologically realistic values

DMD Fast Forward. Published on October 21, 2024 as DOI: 10.1124/dmd.124.001824
This article has not been copyedited and formatted. The final version may differ from this version.

for transporter CLint, intracellular placenta exposure decreased by approximately 10-fold. In this case, an adequate passive diffusion process was maintained to bring drugs to the intracellular compartment. When this process increased by 10-fold (Figure 3), the impact of the efflux transporters became smaller, leading to only 2-fold lower exposure in both placental and umbilical cord. On the other hand, when the passive diffusion reduced by 10-fold, the impact of placental transporters become more pronounced leading to about 30-fold lower exposure in the placenta and umbilical cord. These results indicate that placental efflux transporters can be of clinical significance in reducing fetal exposure and that higher fetal drug levels may be expected if their function is inhibited by, for instance, drug-drug interactions.

Inclusion of patient variability on transporter level is also another advantage of the PBPK-IVIVE combination. This can identify the theoretically conceivable extremes in order to protect the most vulnerable individuals by setting the criteria of exposure based on these cases rather than the average patient. Knowledge on abundance of key drug transporters in placental tissue and placenta cell models is necessary to adequately interpret and extrapolate experimental transport data. Integration of this information in pregnancy-PBPK modeling offers a promising tool to investigate maternal, placental and fetal drug exposure.

Acknowledgments

The authors thank the Biological Mass Spectrometry Core Facility (BioMS), Drs David Knight and Stacey Warwood, at the University of Manchester, for access to mass spectrometry instrumentation. The authors also thank Radboud University Medical Center, Nijmegen, Netherlands for access to placenta samples. This work was supported by Simcyp Grant and Partnership Scheme 2015/16 (Certara®).

Data availability statement

The authors declare that all the data supporting the findings of this study are contained within the paper.

Author contributions

Participated in research design: Z.M.A.-M., J.J.M.-F., R.G, and A.R.-H.

Conducted experiments: Z.M.A.-M., J.J.M.-F., J.V.D.-H and B.A.

Contributed new reagents or analytic tools: Z.M.A.-M.

Performed data analysis: Z.M.A.-M., J.J.M.-F, and K. A.

Wrote or contributed to the writing of the manuscript: Z.M.A.-M., J.J.M.-F., A.C., J.V.D.-H., J.K., K. A., B. A., J.B., R.G., and A.R-H.

References

K. Abduljalil and R.K.S. Badhan, Drug dosing during pregnancy-opportunities for physiologically based pharmacokinetic models, *J Pharmacokinet Pharmacodyn* **47** (2020), pp. 319-340.

K. Abduljalil, P. Furness, T.N. Johnson, A. Rostami-Hodjegan and H. Soltani, **Anatomical, physiological and metabolic changes with gestational age during normal pregnancy: a database for parameters required in physiologically based pharmacokinetic modelling**, *Clin Pharmacokinet* **51** (2012), pp. 365-396.

K. Abduljalil, A. Pansari, J. Ning and M. Jamei, Prediction of Maternal and Fetal Acyclovir, Emtricitabine, Lamivudine, and Metformin Concentrations during Pregnancy Using a Physiologically Based Pharmacokinetic Modeling Approach, *Clin Pharmacokinet* **61** (2022), pp. 725-748.

B. Achour and A. Rostami-Hodjegan, Is Liquid Biopsy Only Restricted to Diagnostics or Can it Go Beyond the Confines of Genotyping and Phenotyping for Quantitative Pharmacology?, *Clin Pharmacol Ther* **112** (2022), pp. 1152-1153.

S. Al-Enazy, S. Ali, N. Albekairi, M. El-Tawil and E. Rytting, Placental control of drug delivery, *Adv Drug Deliv Rev* **116** (2017), pp. 63-72.

Z.M. Al-Majdoub, H. Al Feteisi, B. Achour, S. Warwood, S. Neuhoff, A. Rostami-Hodjegan and J. Barber, Proteomic Quantification of Human Blood-Brain Barrier SLC and ABC Transporters in Healthy Individuals and Dementia Patients, *Mol Pharm* **16** (2019), pp. 1220-1233.

Z.M. Al-Majdoub, D. Scotcher, B. Achour, J. Barber, A. Galetin and A. Rostami-Hodjegan, Quantitative Proteomic Map of Enzymes and Transporters in the Human Kidney: Stepping Closer to Mechanistic Kidney Models to Define Local Kinetics, *Clin Pharmacol Ther* **110** (2021), pp. 1389-1400.

O. Anoshchenko, B. Prasad, N.K. Neradugomma, J. Wang, Q. Mao and J.D. Unadkat, Gestational Age-Dependent Abundance of Human Placental Transporters as Determined by Quantitative Targeted Proteomics, *Drug Metab Dispos* **48** (2020), pp. 735-741.

M.C. Blehar, C. Spong, C. Grady, S.F. Goldkind, L. Sahin and J.A. Clayton, Enrolling pregnant women: issues in clinical research, *Womens Health Issues* **23** (2013), pp. e39-45.

A.M. Carter, Animal models of human pregnancy and placentation: alternatives to the mouse, *Reproduction* **160** (2020), pp. R129-R143.

X. Chang, Y.M. Tan, D.G. Allen, S. Bell, P.C. Brown, L. Browning, P. Ceger, J. Gearhart, P.J. Hakkinen, S.V. Kabadi, N.C. Kleinstreuer, A. Lumen, J. Matheson, A. Paini, H.A. Pangburn, E.J. Petersen, E.N. Reinke, A.J.S. Ribeiro, N. Sipes, L.M. Sweeney, J.F. Wambaugh, R. Wange, B.A. Wetmore and M. Mumtaz, IVIVE: Facilitating the Use of In Vitro Toxicity Data in Risk Assessment and Decision Making, *Toxics* **10** (2022).

J.A. Christopher, A. Geladaki, C.S. Dawson, O.L. Vennard and K.S. Lilley, Subcellular Transcriptomics and Proteomics: A Comparative Methods Review, *Mol Cell Proteomics* **21** (2022), p. 100186.

A. Dallmann, X.I. Liu, G.J. Burckart and J. van den Anker, Drug Transporters Expressed in the Human Placenta and Models for Studying Maternal-Fetal Drug Transfer, *J Clin Pharmacol* **59 Suppl 1** (2019), pp. S70-S81.

E. El-Khateeb, B. Achour, Z.M. Al-Majdoub, J. Barber and A. Rostami-Hodjegan, Non-uniformity of Changes in Drug-Metabolizing Enzymes and Transporters in Liver Cirrhosis: Implications for Drug Dosage Adjustment, *Mol Pharm* **18** (2021), pp. 3563-3577.

G.A.M. Eliesen, H. van Hove, M.H. Meijer, P.H.H. van den Broek, J. Pertijs, N. Roeleveld, J. van Drongelen, F.G.M. Russel and R. Greupink, Toxicity of anticancer drugs in human placental tissue explants and trophoblast cell lines, *Arch Toxicol* **95** (2021), pp. 557-571.

S. Gil, R. Saura, F. Forestier and R. Farinotti, P-glycoprotein expression of the human placenta during pregnancy, *Placenta* **26** (2005), pp. 268-270.

L. Goetzl, N. Darbinian, N. Merabova, L.C. Devane and S. Ramamoorthy, Gestational Age Variation in Human Placental Drug Transporters, *Front Pharmacol* **13** (2022), p. 837694.

C. Gong, L.N. Bertagnolli, D.W. Boulton and P. Coppola, A Literature Review of Changes in Phase II Drug-Metabolizing Enzyme and Drug Transporter Expression during Pregnancy, *Pharmaceutics* **15** (2023).

P.L. Grigsby, Animal Models to Study Placental Development and Function throughout Normal and Dysfunctional Human Pregnancy, *Semin Reprod Med* **34** (2016), pp. 11-16.

L.W. Han, C. Gao and Q. Mao, An update on expression and function of P-gp/ABCB1 and BCRP/ABCG2 in the placenta and fetus, *Expert Opin Drug Metab Toxicol* **14** (2018), pp. 817-829.

M.D. Harwood, B. Achour, S. Neuhoff, M.R. Russell, G. Carlson, G. Warhurst and A. Rostami-Hodjegan, In Vitro-In Vivo Extrapolation Scaling Factors for Intestinal P-glycoprotein and Breast Cancer Resistance Protein: Part II. The Impact of Cross-Laboratory Variations of Intestinal Transporter Relative Expression Factors on Predicted Drug Disposition, *Drug Metab Dispos* **44** (2016), pp. 476-480.

M.D. Harwood, A. Rostami-Hodjegan and S. Neuhoff, Application of Physiologically Based Pharmacokinetic and Pharmacodynamic (Pbpk/Pd) Modeling Comprising Transporters. *Drug Transporters* (2022), pp. 475-496.

M. Iqbal, M.C. Audette, S. Petropoulos, W. Gibb and S.G. Matthews, Placental drug transporters and their role in fetal protection, *Placenta* **33** (2012), pp. 137-142.

A.K. Kammala, R.C.V. Lintao, N. Vora, A. Mosebarger, K. Khanipov, G. Golovko, J.L. Yaklic, M.R. Peltier, T.P. Conrads and R. Menon, Expression of CYP450 enzymes in human fetal membranes and its implications in xenobiotic metabolism during pregnancy, *Life Sci* **307** (2022), p. 120867.

A.B. Ke, R. Greupink and K. Abduljalil, Drug Dosing in Pregnant Women: Challenges and Opportunities in Using Physiologically Based Pharmacokinetic Modeling and Simulations, *CPT Pharmacometrics Syst Pharmacol* **7** (2018), pp. 103-110.

H. Li, B. van Ravenzwaay, I.M. Rietjens and J. Louisse, Assessment of an in vitro transport model using BeWo b30 cells to predict placental transfer of compounds, *Arch Toxicol* **87** (2013), pp. 1661-1669.

A. Lupattelli, O. Spigset, M.J. Twigg, K. Zagorodnikova, A.C. Mardby, M.E. Moretti, M. Drozd, A. Panchaud, K. Hameen-Anttila, A. Rieutord, R. Gjergja Juraski, M. Odalovic, D. Kennedy, G. Rudolf, H. Juch, A. Passier, I. Bjornsdottir and H. Nordeng, Medication use in pregnancy: a cross-sectional, multinational web-based study, *BMJ Open* **4** (2014), p. e004365.

A.A. Mathias, J. Hitti and J.D. Unadkat, P-glycoprotein and breast cancer resistance protein expression in human placentae of various gestational ages, *Am J Physiol Regul Integr Comp Physiol* **289** (2005), pp. R963-969.

H.E. Meyer zu Schwabedissen, M. Grube, A. Dreisbach, G. Jedlitschky, K. Meissner, K. Linnemann, C. Fusch, C.A. Ritter, U. Volker and H.K. Kroemer, Epidermal growth factor-mediated activation of the map kinase cascade results in altered expression and function of ABCG2 (BCRP), *Drug Metab Dispos* **34** (2006), pp. 524-533.

C. Monti, M. Zilocchi, I. Colugnat and T. Alberio, Proteomics turns functional, *J Proteomics* **198** (2019), pp. 36-44.
H. Msheik, S. El Hayek, M.F. Bari, J. Azar, W. Abou-Kheir, F. Kobeissy, M. Vatish and G. Daoud, Transcriptomic profiling of trophoblast fusion using BeWo and JEG-3 cell lines, *Mol Hum Reprod* **25** (2019), pp. 811-824.
M. Nishimura and S. Naito, Tissue-specific mRNA expression profiles of human ATP-binding cassette and solute carrier transporter superfamilies, *Drug Metab Pharmacokinet* **20** (2005), pp. 452-477.
B. Prasad, B. Achour, P. Artursson, C. Hop, Y. Lai, P.C. Smith, J. Barber, J.R. Wisniewski, D. Spellman, Y. Uchida, M.A. Zientek, J.D. Unadkat and A. Rostami-Hodjegan, Toward a Consensus on Applying Quantitative Liquid Chromatography-Tandem Mass Spectrometry Proteomics in Translational Pharmacology Research: A White Paper, *Clin Pharmacol Ther* **106** (2019), pp. 525-543.
T. Rodgers and M. Rowland, Physiologically based pharmacokinetic modelling 2: predicting the tissue distribution of acids, very weak bases, neutrals and zwitterions, *J Pharm Sci* **95** (2006), pp. 1238-1257.
M.R. Russell, B. Achour, E.A. McKenzie, R. Lopez, M.D. Harwood, A. Rostami-Hodjegan and J. Barber, Alternative fusion protein strategies to express recalcitrant QconCAT proteins for quantitative proteomics of human drug metabolizing enzymes and transporters, *J Proteome Res* **12** (2013), pp. 5934-5942.
H. Schneider, C. Albrecht, M.S. Ahmed, M. Broekhuizen, L. Aengenheister, T. Buerki-Thurnherr, A.H.J. Danser, S. Gil, S.R. Hansson, R. Greupink, R.M. Lewis, U.R. Markert, L. Mathiesen, N. Powles-Glover, C. Wadsack and P. Brownbill, Ex vivo dual perfusion of an isolated human placenta cotyledon: Towards protocol standardization and improved inter-centre comparability, *Placenta* **126** (2022), pp. 83-89.
F. Staud, L. Cerveny and M. Ceckova, Pharmacotherapy in pregnancy; effect of ABC and SLC transporters on drug transport across the placenta and fetal drug exposure, *J Drug Target* **20** (2012), pp. 736-763.
M. Sun, J. Kingdom, D. Baczyk, S.J. Lye, S.G. Matthews and W. Gibb, Expression of the multidrug resistance P-glycoprotein, (ABCB1 glycoprotein) in the human placenta decreases with advancing gestation, *Placenta* **27** (2006), pp. 602-609.
A.M. Vasilogianni, E. El-Khateeb, B. Achour, S. Alrubia, A. Rostami-Hodjegan, J. Barber and Z.M. Al-Majdoub, A family of QconCATs (Quantification conCATemers) for the quantification of human pharmacological target proteins, *J Proteomics* **261** (2022), p. 104572.
H.G. Wittgen, R. Greupink, J.J. van den Heuvel, P.H. van den Broek, H. Dinter-Heidorn, J.B. Koenderink and F.G. Russel, Exploiting transport activity of p-glycoprotein at the blood-brain barrier for the development of peripheral cannabinoid type 1 receptor antagonists, *Mol Pharm* **9** (2012), pp. 1351-1360.
Z. Zhang, M.Z. Imperial, G.I. Patilea-Vrana, J. Wedagedera, L. Gaohua and J.D. Unadkat, Development of a Novel Maternal-Fetal Physiologically Based Pharmacokinetic Model I: Insights into Factors that Determine Fetal Drug Exposure through Simulations and Sensitivity Analyses, *Drug Metab Dispos* **45** (2017), pp. 920-938.
Z. Zhang and J.D. Unadkat, Development of a Novel Maternal-Fetal Physiologically Based Pharmacokinetic Model II: Verification of the model for passive placental permeability drugs, *Drug Metab Dispos* **45** (2017), pp. 939-946.

Footnotes

This work is funded by Simcyp Grant and Partnership Scheme 2015/16 (Certara®).

A. Rostami-Hodjegan and K. Abduljalil are employees of Certara Ltd., a provider of modelling and simulation platforms to academic and industrial institutions. The other authors declare no competing interests.

Figure Legends

Figure 1. Expression levels and the mean (red bars) of P-gp, BCRP (A) and MRPs (B) in membrane fraction derived from human placentae at term (n=5, 3 sites each), as determined by QconCAT based-targeted proteomics approach. Each point represents 1 site from each individual placenta.

Figure 2. Concentration of a hypothetical compound in maternal plasma, intracellular placenta, and umbilical vein plasma over time without (left) and with (right) efflux transporter kinetics that efflux drug out of the placenta back to maternal circulation. Bottom plots are for the cord-to-maternal ratio. Insets show the same plots but with adjusted y-axis for clarity. Solid line represents the simulated mean and dashed lines represent the simulated 5^{th} and 95^{th} percentiles. Abbreviation: IC, intracellular.

Figure 3. Sensitivity analysis for the impact of passive diffusion clearance (assumed to be 0.005 mL/h/ mL of placental volume) on maternal, placenta, and umbilical venous exposure. Value was set at 10-fold higher and lower. Abbreviation: CLPDM, placental passive diffusion clearance from maternal side to placenta.

DMD Fast Forward. Published on October 21, 2024 as DOI: 10.1124/dmd.124.001824
This article has not been copyedited and formatted. The final version may differ from this version.

Tables

Table 1: Protein expression (pmol/mg total membrane protein) of ATP-binding cassette (ABC) transporters and basal plasma membrane marker (Na^+/K^+ ATPase) obtained from human placentae (n=5) at term, sampled at 3 different sites of each placenta (1: near umbilical cord, 2: mid placenta, 3: outer placenta)

Site	P-gp	BCRP	MRP2	MRP3	MRP4	MRP6	Na^+/K^+ATPase
Placenta 1							
Site 1	0.16	0.15	0.25	0.16	0.11	0.10	0.61
Site 2	0.33	0.32	0.23	0.28	0.22	0.28	1.79
Site 3	0.15	0.29	0.15	0.15	0.11	0.10	2.29
Mean	**0.21**	**0.25**	**0.21**	**0.20**	**0.15**	**0.16**	**1.56**
SD	**0.10**	**0.09**	**0.05**	**0.07**	**0.06**	**0.10**	**0.86**
% CV	**47.4**	**35.8**	**25.2**	**36.8**	**43.3**	**64.9**	**55.2**
Placenta 2							
Site 1	0.26	0.23	0.24	0.25	0.18	0.17	1.09
Site 2	0.21	0.23	0.16	0.20	0.14	0.13	1.07
Site 3	0.14	0.14	0.13	0.15	0.09	0.11	0.96
Mean	**0.20**	**0.20**	**0.18**	**0.20**	**0.14**	**0.14**	**1.04**
SD	**0.06**	**0.05**	**0.06**	**0.05**	**0.05**	**0.03**	**0.07**
% CV	**29.6**	**26.0**	**32.2**	**25.0**	**33.0**	**22.3**	**6.73**
Placenta 3							
Site 1	0.12	0.16	0.10	0.12	0.10	0.07	1.23
Site 2	0.20	0.32	0.21	0.19	0.18	0.13	4.97
Site 3	0.19	0.15	0.18	0.17	0.13	0.12	1.95
Mean	**0.17**	**0.21**	**0.16**	**0.16**	**0.14**	**0.11**	**2.72**
SD	**0.04**	**0.09**	**0.06**	**0.04**	**0.04**	**0.03**	**1.98**
% CV	**25.6**	**45.4**	**34.8**	**22.5**	**29.6**	**30.1**	**73.0**
Placenta 4							
Site 1	0.12	0.11	0.07	0.08	0.05	0.04	0.83
Site 2	0.30	0.16	0.11	0.11	0.08	0.07	0.79
Site 3	0.18	0.17	0.08	0.09	0.07	0.05	1.19
Mean	**0.20**	**0.15**	**0.09**	**0.09**	**0.07**	**0.05**	**0.94**
SD	**0.09**	**0.03**	**0.02**	**0.02**	**0.02**	**0.02**	**0.22**
% CV	**45.8**	**21.9**	**24.0**	**16.4**	**22.9**	**28.6**	**23.5**
Placenta 5							
Site 1	0.10	0.07	0.06	0.07	0.03	0.04	0.88
Site 2	0.34	0.24	0.27	0.26	0.20	0.20	3.53
Site 3	0.13	0.11	0.09	0.08	0.05	0.06	1.26
Mean	**0.19**	**0.14**	**0.14**	**0.14**	**0.09**	**0.10**	**1.89**
SD	**0.13**	**0.09**	**0.11**	**0.11**	**0.09**	**0.09**	**1.43**

% CV	**68.8**	**63.5**	**81.1**	**78.2**	**99.6**	**87.2**	**75.8**

BCRP, breast cancer resistance protein; %CV, coefficient of variation; MRP, multi-drug resistance protein; P-gp, P-glycoprotein; SD, standard deviation

Table 2. Expression (pmol/mg membrane protein, mean ± SD, n = 3) of P-gp and BCRP in HEK293, BeWo and BeWo b30, JEG-3 and in membrane vesicles derived of HEK293 cells overexpressing the indicated transporters as determined by QconCAT-based targeted proteomics. * Ratio (in vitro expression/tissue expression) is based on the mean of transporter expression in n = 3 placentae and n = 3 batches of vesicle/cells (model systems). These *ratios should be considered as indicative rather than absolute as they are based on the assumption of consistent protein yields, across different systems due to the use of different extraction methods. BLQ: below limit of quantification NA: not available (because of BLQ expression levels in BeWo cells).

Cell line	**Protein**	**Batch 1**	**Batch 2**	**Batch 3**	**Overall mean (3 batches)**	**Model system / placentae expression ***
		Expression (pmol/mg) Mean ± SD				
HEK293						
Overexpressing P-gp	P-gp	8.84 ± 0.58	3.07 ± 0.19	6.17 ±2.24	6.03 ± 2.89	31.74
Overexpressing BCRP	BCRP	-	1.09 ± 0.40	4.94 ± 4.0	3.02 ± 2.72	15.89
Trophoblast cell line						
BeWo	P-gp	BLQ				NA
	BCRP	BLQ				NA
BeWo b30	P-gp	0.26 ± 0.22				1.37
	BCRP	2.94 ± 2.54				15.47
JEG-3	P-gp	0.14 ± 0.17				0.74
	BCRP	0.99 ± 0.89				5.21
Membrane vesicles						
Overexpressing P-gp	P-gp	4.9 ± 3.45	3.80 ± 0.45	5.0 ± 0.80	4.57 ± 0.67	24.05
Overexpressing BCRP	BCRP	5.2 ± 0.91	22.1 ± 2.67	15.9 ± 1.17	14.4 ± 8.55	75.79

DMD Fast Forward. Published on October 21, 2024 as DOI: 10.1124/dmd.124.001824
This article has not been copyedited and formatted. The final version may differ from this version.

Table 3. Transport of model substrates NMQ (for P-gp) or E1S (for BCRP) in various batches of membrane vesicles overexpressing P-gp or BCRP. The vesicle batches correspond to those analyzed for transporter abundance using proteomics. Transport rates are expressed per mg of total vesicular (crude membrane) protein. Transport was assessed both in presence and absence of ATP, to assess ATP-dependency of transport in the presence of 0.1 µM (0.1 pmol/µl) of the substrates.

Overexpressed Transporter	**Batch Number**	**Transport of substrate in presence of ATP**	**Transport substrate in absence of ATP**
		Mean ± SD	Mean ± SD
		(pmol/mg protein/min)	(pmol/mg protein/min)
P-gp	1	19.4 ± 0.08	3.11 ± 0.26
	2	23.3 ± 0.20	2.77 ± 0.08
	3	25.3 ± 0.66	2.98 ± 0.28
BCRP	1	8.08 ± 0.90	0.79 ± 0.23
	2	16.8 ± 0.29	0.25 ± 0.00
	3	54.8 ± 1.75	0.69 ± 0.18

DMD Fast Forward. Published on October 21, 2024 as DOI: 10.1124/dmd.124.001824
This article has not been copyedited and formatted. The final version may differ from this version.

Table 4. Input parameters for the Simcyp model (hypothetical drug)

Parameter	Unit	Value
Physicochemical properties		
Molecular weight	g/mol	129.16
log $P_{o:w}$	dimensionless	-0.43
Compound Type	dimensionless	Monoprotic Base
pKa 1	Dimensionless	11.8
Plasma fu	Dimensionless	1
B/P	Dimensionless	1
Distribution		
Model	Full PBPK model	
Vss	L/kg	Predicted using Rodgers & Rowland method (Rodgers and Rowland, 2006)
Elimination		
CLint (CYP3A4)	µL/min/pmol	0.5
Placental model		
CL_{PDM}	L/h/mL placenta	0.005
CL_{PDF}	L/h/mL placenta	0.005
CLu_{int}_P-gp	µL/min/pmol transporter	95.8
fu_{inc} (P-gp)	Dimensionless	1
ISEF (P-gp)	Dimensionless	1
CLu_{int}_BCRP	µL/min/pmol transporter	36.2
fu_{inc} (BCRP)	Dimensionless	1
ISEF (BCRP)	Dimensionless	1
System Parameters		
Absolute Abundance (P-gp)	pmol / g placental tissue	5.27
Absolute Abundance (BCRP)	pmol / g placental tissue	5.16

BCRP, breast cancer resistance protein; B/P, blood to plasma partition coefficient; CL_{PDM}, placenta placental permeability clearance from maternal side to placenta; CL_{PDF}, placental passive permeability clearance from fetal side to placenta; CL_{int}, intrinsic clearance; CLU_{int}, unbound intrinsic clearance; CYP3A4, cytochrome P450 3A4; fu, fraction unbound; fu_{inc}, free fraction of the drug in the in vitro incubation system; ISEF, intersystem extrapolation factor; P-gp, P-glycoprotein; V_{ss}, volume of distribution at steady state.

Figure 1

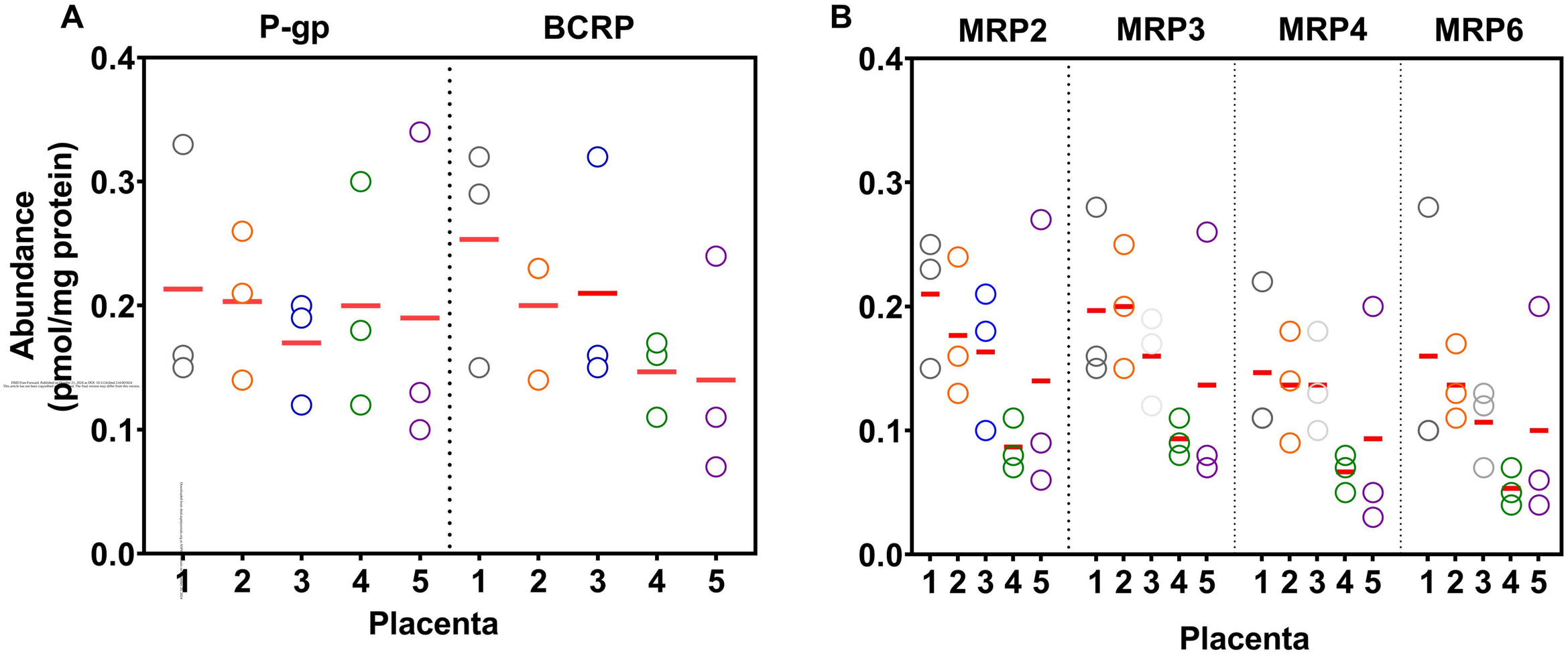

Figure 2

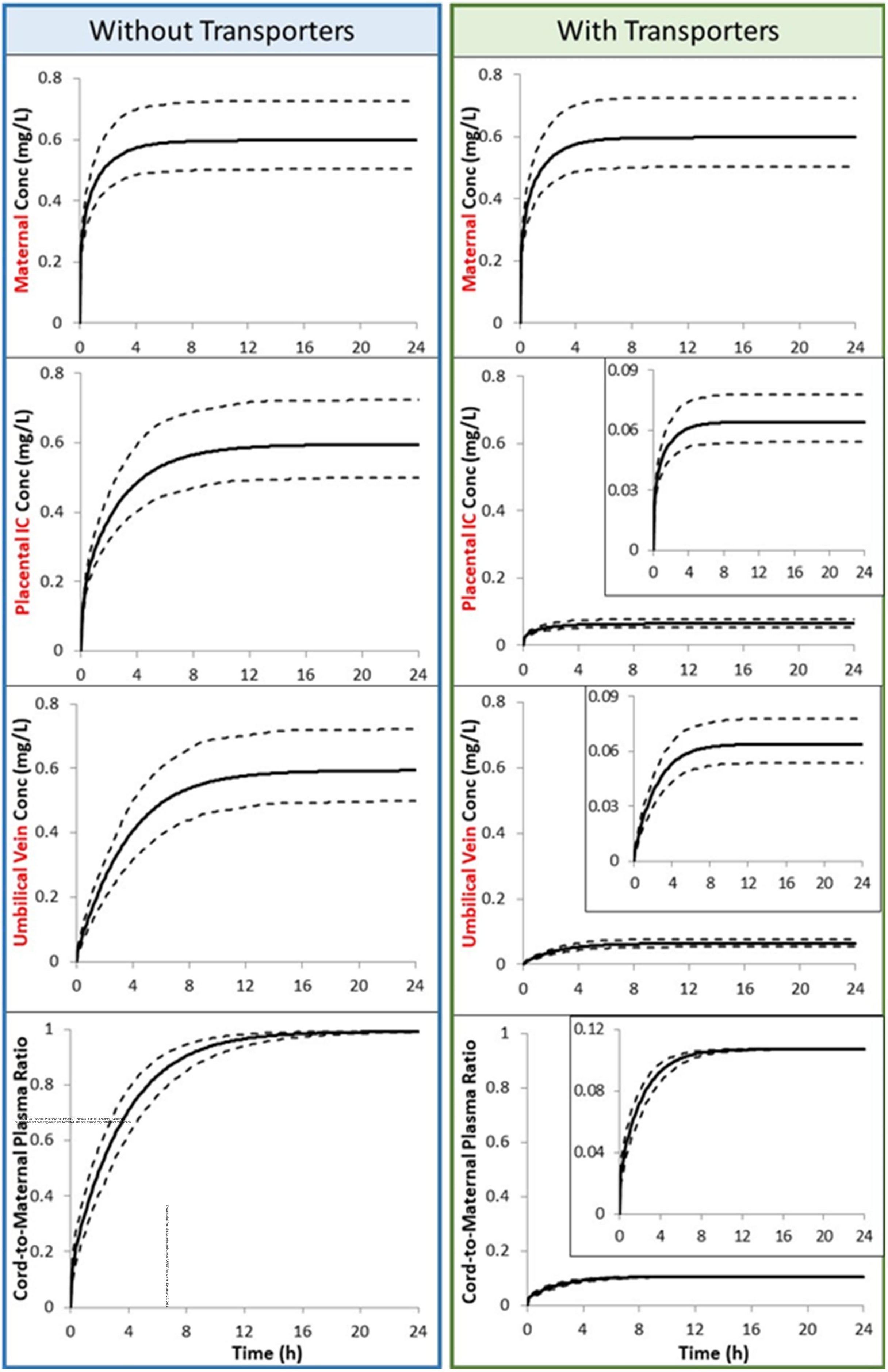

Figure 3